Material characterisation for Finite Element simulations of draping with non-crimp fabrics

R.H.W. ten Thije, R. Loendersloot, R. Akkerman

University of Twente, Twente Institute of Mechanics
P.O. Box 217 – 7500 AE Enschede – the Netherlands
URL: www.composites.ctw.utwente.nl
e-mail: R.H.W.tenThije@ctw.utwente.nl

ABSTRACT: The draping process of non-crimp fabrics (NCFs) determines the fibre distribution and hence the NCF composite processing and performance. An efficient Finite Element (FE) model is being developed to model this draping process. The work presented in this paper is the first step in the development of this FE model of the draping process of the NCF on the mould. The NCF material behaviour is characterised in a continuum representation. The primary deformation mechanisms are identified. Appropriate constitutive relations are proposed and experiments are presented by which the necessary material constants can be obtained.

Key words: NCF, draping, material characterisation, deformation mechanisms

1 INTRODUCTION

Processability and performance are conflicting aspects in the development of resin infused non-crimp fabric (NCF) based composites. Easily drapeable and easily infusible NCFs often result in poor mechanical performance and vice versa. An optimum can be found by modelling both processing and performance. For components exhibiting double curvature, the process of draping the NCF on the mould plays a key role. The fibre distribution after draping dominates both the filling process and the mechanical performance of the finished part.
In the current project a Finite Element (FE) model will be developed to simulate the draping process of NCFs on arbitrary geometries. The model has to identify problem areas during the draping and it has to determine the fibre distribution in the final NCF. This paper describes the first step in the development of the FE model: the identification of the main deformation mechanisms of the NCF unit cell. In this case:

1. Extension and compaction of the stitch material
2. Compaction of the yarns (during shear deformation)
3. Rotation of the yarns
4. Sliding of the yarns

The deformation mechanisms are described in a continuum formulation, based on semi-empirical laws. The second step will be the implementation of the mechanical behaviour of a multidirectional NCF into a single membrane element. This will enable efficient FE simulations of the NCF draping process. The possibility of the individual yarns to slide through the stitches is an unconventional part of the deformation, when comparing with the more common woven fabrics. The next sections describe the modelling of the NCF materials and the deformation mechanisms. Experiments will be specified to obtain the necessary material constants.

2 MATERIAL AND MODELLING

The NCFs used in this project are biaxial chain knitted $^{+}/_{-}$ 45° fabrics with a polyester stitch thread. Both glass and carbon fibre based fabrics are used.

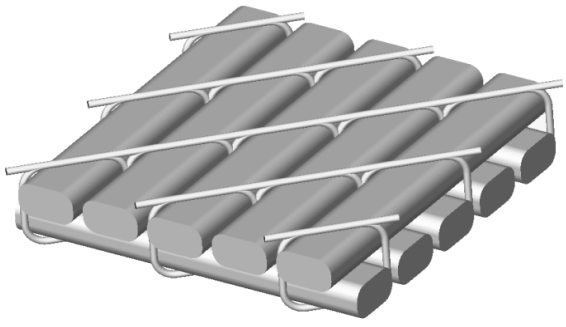

Fig. 1. Local element model.

Figure 1 shows a small, idealised area of the NCF. The assumption is made that the fabric consists of yarns, which are oriented parallel to each other. The stitches are represented by a continuous fibre, which is wrapped around the yarns of the top and the bottom layer. A small amount of fibres runs from one yarn into the adjacent yarns. This will be ignored for the sake of convenience.

3 DEFORMATION MECHANISMS

3.1 Stitch extension

The stitches dominate the mechanical behaviour if the NCF is stretched in the direction of the stitches. At zero deformation, the stitch is not completely stretched. Its stiffness will therefore be very low at this point. The stitch becomes stretched at a certain strain and the stiffness will increase to a higher value. Figure 2 shows the results of a tensile test of the two fabrics in the direction of the stitches.

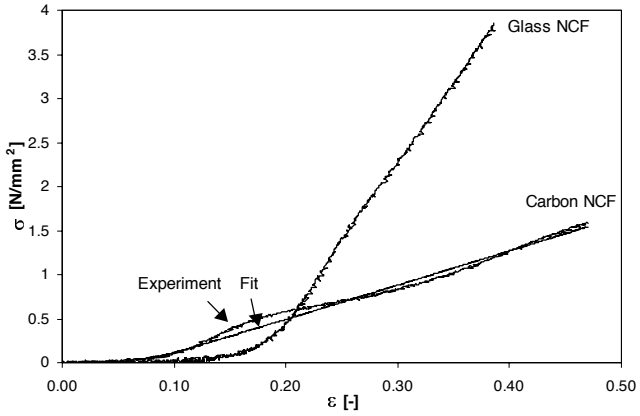

Fig. 2. Tensile test in the direction of the stitches. Fit: E_s = 3.89 [MPa], b_s = 26.0 [-], ε_{0s} = 0.073 [-]

The stiffness of the stitches is modelled by an equivalent Young's modulus in the direction of the stitches. It is assumed that the stiffness under compression is zero. The initial stiffness during extension is low and increases to the equivalent stiffness E_s beyond the point where the stitches are completely stretched. A suitable function to describe the tangent of a one dimensional stress-strain function is given by:

$$\frac{d\sigma_s}{d\varepsilon} = E_s\left(\frac{1}{1+10^{b_s(\varepsilon_{0s}-\varepsilon)}}\right), \tag{1}$$

where σ_s and ε are the one-dimensional stress and strain in the direction of the stitch, E_s is the Young's modulus if the fibres are stretched, ε_{0s} is the stretching point and b_s is the slope at the stretching point. Integration of this function results in an appropriate stress-strain function.

The stress contribution of the stitches in a continuum representation of the fabric is obtained by the following analysis.

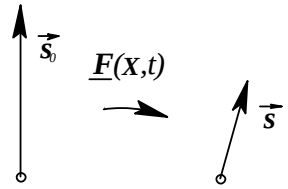

Fig. 3. Deformation of the stitch.

Figure 3 shows a deformation of a vector representing a stitch in a continuous body. The new stitch vector $\vec{s}$ can be found by $\vec{s} = \underline{F}(X,t)\cdot\vec{s}_0$, with $\underline{F}(X,t)$ the deformation gradient and $\vec{s}_0$ the original stitch vector. The strain in the stitch is calculated by:

$$\varepsilon = \frac{\|\vec{s}\|}{\|\vec{s}_0\|} - 1. \tag{2}$$

With the one-dimensional strain and equation (1) the stress σ_s in the direction of $\vec{s}$ can be calculated. The elastic stress contribution of the stitches to the total stress tensor can be obtained by:

$$\underline{\sigma}_S = \sigma_S \vec{s}^{*}\vec{s}^{*}, \tag{3}$$

where $\vec{s}^{*}$ is the normalized vector of $\vec{s}$.

Figure 2 shows a least squares fit of the material constants on the experimental results from the tensile test of the carbon NCF.

3.2 Yarn compaction

The yarns are compacted during shear deformation of the fabric, due to the decrease in surface area in a pure 'trellis' deformation. This inplane compaction of the yarns is modelled with a stiffness transverse to the yarns.

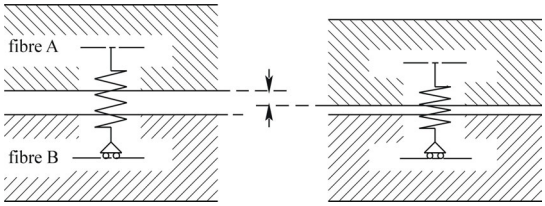

Fig. 4. Yarn compaction model.

The inplane compression response is non-linear. Initially the stiffness is low. The yarns redistribute and fill the open spaces when they are compacted. The stiffness increases significantly at the point where the yarns are completely pressed together. A similar description as (1) is employed to describe this behaviour, but here the stiffness is built up during compression. The strain transverse to the fibres is calculated with the following vectors:

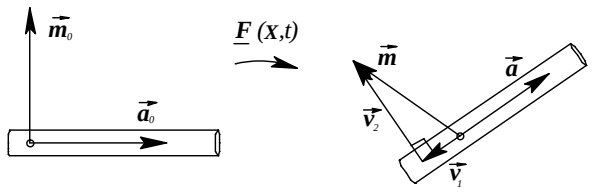

Fig. 5. Compression of the yarns.

$\vec{a}_0$ is the initial fibre vector and $\vec{m}_0$ is a vector initially perpendicular to this fibre. $\vec{a}$ and $\vec{m}$ are the same vectors after deformation. The resulting strain transverse to the fibres is now calculated by:

$$\varepsilon = \frac{\|\vec{v}_2\|}{\|\vec{m}_0\|} - 1, \tag{4}$$

where $\vec{v}_1$ and $\vec{v}_2$ can be obtained by simple vector operations: $\vec{v}_2 = \vec{m} - \vec{v}_1$ and $\vec{v}_1 = (\vec{m} \cdot \vec{a})\vec{a}$. The elastic stress contribution of the compaction of the yarns to the total stress tensor can be obtained by:

$$\underline{\sigma}_c = \sigma_c \vec{v}_2^{\,*} \vec{v}_2^{\,*}, \tag{5}$$

where $\vec{v}_2^{\,*}$ is the normalized vector of $\vec{v}_2$.

The parameters describing the compression response are determined simultaneously with the yarn rotation response.

3.3 Yarn rotation

The yarns of the top and bottom layer rotate with respect to each other during shear deformation. This introduces friction. The friction can be measured with a trellis frame experiment. The experiment is in line with the experiments presented by Spencer in [1], which also describes the deformation and orientation of the fibres. In the current analysis elastic effects play a role, instead of viscous. A relation between stresses, strains and force on the trellis frame can be obtained by equating the internal work to the external work, equation (6) and (7).

$$W_{\text{ext}} = 2\left(\tfrac{1}{2}\delta \cdot F\right) = F \cdot l\left(\cos\phi - \cos\phi_0\right) \tag{6}$$

$$W_{\text{int}} = \tfrac{1}{2}\left(\sigma_{11}\varepsilon_{11} + \sigma_{22}\varepsilon_{22} + 2\sigma_{12}\varepsilon_{12}\right) l^2 h \sin(2\phi) \tag{7}$$

where F, δ and ϕ can be found in figure 6, l is the length of the trellis frame arm and h is the current thickness of the fabric.

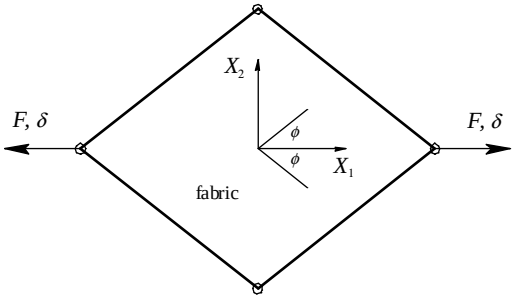

Fig. 6. Trellis frame experiment.

Figure 7 shows the results of the trellis frame experiment on the glass and the carbon NCF. The NCFs show a rather flat loading curve during the first part of the trellis frame deformation. This is due to the friction between the rotating yarns. The compaction of the yarns starts to dominate at shear angles above 40 to 50 degrees.

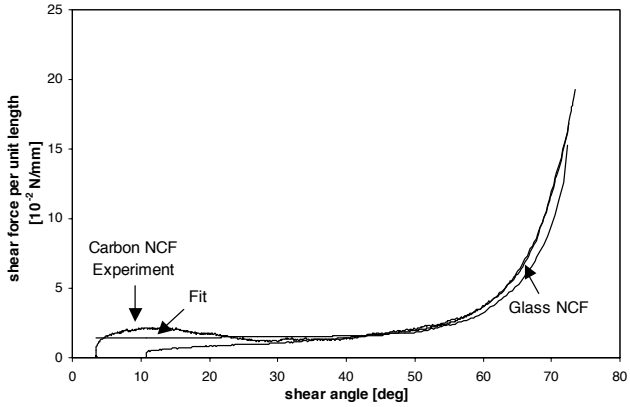

Fig. 7. Trellis frame experiment with NCF fabrics.

The experiment with the carbon NCF was repeated at different velocities to find out whether the friction is of a Coulomb type or viscous. The results can be found in table 1. These results indicate that the friction is mainly of a Coulomb type.

Table 1. Shear force at different velocities experiment.

Test speed [mm/min]	Shear force per unit length [10^{-2} N/mm]
10	0.64
50	0.89
100	0.79
500	0.75
999	0.72

The shear force can be represented by a constant μ.

Figure 8 shows how the friction is implemented in the continuous representation.

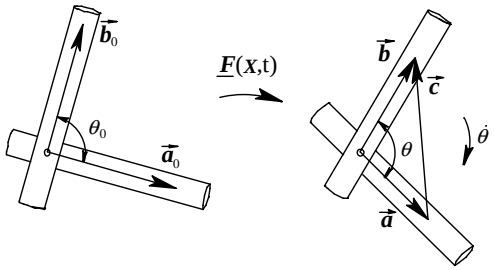

Fig. 8. Rotation of the yarns.

$\vec{a}_0$ and $\vec{b}_0$ are the initial fibre vectors in the two layers. A stress is applied in the direction of $\vec{c}$ for a non-zero $\dot{\theta}$. The contribution to the total stress tensor can be calculated by:

$$\underline{\sigma}_r = \sigma_r \vec{c}^* \vec{c}^*, \qquad \text{with } \sigma_r = \text{sgn}(\dot{\theta})\mu \tag{8}$$

Figure 7 shows a least squares fit on the experiment with the carbon NCF, including the yarn compaction response and the friction response. The volume is considered constant as a first approximation.

3.4 Sliding of the yarns

The individual yarns can slide through the stitches in their own longitudinal direction. Every stitch is interpreted as an obstacle, which introduces friction. Figure 9a shows a possible setup to measure the friction coefficient during the sliding of the yarns.

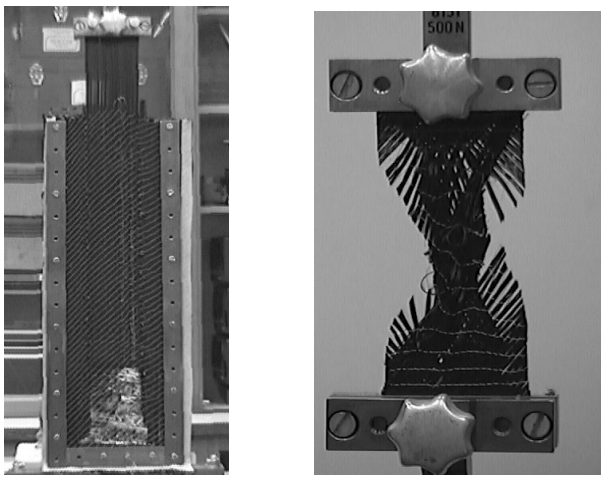

Fig. 9a and 9b. Fibre pull-out and bias extension experiment.

The stitches are tensioned during the fibre pull-out test. This results in a significant increase of the tensile forces in the pulled out fibres. Only friction coefficients at a high stitch tension can be obtained. Extrapolation to the properties at lower stitch tensions is susceptible to large errors. The friction coefficients at low stitch tensions can also be obtained by a bias extension experiment. This experiment can be seen in figure 9b. Isolating the effects of the sliding yarns is difficult in this case, because the fabric shows large shear deformations. The stress contribution of the sliding fibres in a continuum representation is given by:

$$\underline{\sigma}_{sl} = \sigma_{sl}(v, \sigma_s)\vec{a}^*\vec{a}^* \tag{9}$$

where the scalar σ_{sl} depends on at least the sliding velocity of the yarns and the stitch tension. The vector $\vec{a}$ is the fibre vector, the only direction in which the yarn can move.

4 FUTURE WORK

The NCF–typical modes of deformation will be implemented in a previously developed extension of Spencer's fabric reinforced fluid model [1], [2] which simulates the draping of woven fabrics. Although the theory is based on a fluid model, the viscous contribution is small. The multidirectional fabric will be modelled as a single anisotropic continuum.

5 CONCLUSIONS

An existing model for drape analysis of woven fabrics will be extended for typical NCF behaviour. The local modelling is going hand-in-hand with experimental characterisation of the drape behaviour. It is shown that the material properties can be determined by performing and evaluating four different experiments.

ACKNOWLEDGEMENTS

This work was performed with the support from the European Commission, by means of the FALCOM project (GRD1-2001-40184). This support is gratefully acknowledged by the authors.

REFERENCES

1. A.J.M. Spencer, *Theory of fabric-reinforced viscous fluids*, University of Nottingham, Nottingham (2000). In: *Composites: Part A*, vol. 31, 2000, p.1311-1321.
2. E.A.D. Lamers et al., *Fibre Orientation Modelling for Rubber Press Forming of Thermoplastic Laminates*, University of Twente, Enschede (2002) In: *Proc. ESAForm*, eds, M. Pietrzyk, Z. Mitura, J. Kaczmar (2002), p. 323-326.